II International Conference on Particle-based Methods - Fundamentals and Applications
PARTICLES 2011
E. Oñate and D.R.J. Owen (Eds)

NUMERICAL SIMULATIONS OF GRANULAR MEDIA COMPOSED WITH IRREGULAR POLYHEDRAL PARTICLES: EFFECT OF PARTICLES' ANGULARITY

E. Azéma*, F. Radjai*, F. Dubois*

*LMGC, CNRS-Universit Montpellier 2, Montpellier, France.
emilien.azema@univ-montp2.fr, frederic.dubois@univ-montp2.fr, franck.radjai@univ-montp2.fr

Key words: Granular Materials, particle shape, angularity, texture, force transmission

Abstract. We use contact dynamic simulations to perform a systematic investigation of the effects of particles shape angularity on mechanicals response in sheared granular materials. The particles are irregular polyhedra with varying numbers of face from spheres to "double pyramid" shape with a constant aspect ratio. We study the quasi-static behavior, structural and force anisotropies of several packings subjected to triaxial compression. An interesting finding is that the shear strength first increases with angularity up to a maximum value and then saturates as the particles become more angular. Analyzing the anisotropies induced by the angular distributions of contacts and forces orientations, we show that the saturation of the shear strength at higher angularities is a consequence of fall-off of the texture anisotropies compensated by an increase of the tangential force anisotropy. This is attributed to the fact that at higher angularity, particles are better connected (or surrounded) leading to an increase of friction mobilization in order to achieve the deformation. Moreover, the most angular particles also have very few sides so that, this effect is enhanced by the increase of the proportion of face-side and side-side contacts with angularity.

1 INTRODUCTION

One of the way to build a clearer picture of the complex behavior exhibited by real granular materials, is to understand and quantify the effects of grain shape. As shown experimentally and numerically by various author, angular[3, 7], elongated [4, 9] or non-convex [10] shapes, strongly affect the shear strength and the solid fraction, as well as the microstructure of the material. For example, they shows that this influence is sometimes counterintuitive, as in the case of the correlation between the elongation or the non-convexity of the grains and the solid fraction of the packing [4, 9, 10].

Nevertheless, a systematic and quantitative investigation of particle shape effect is still elusive because of three major difficulties: 1) Particle shape can be described in

terms of several parameters as angularity, elongation, flattening, non-convexity... 2) Each parameters need to be defined conveniently in order to be able to generate particle shapes with continuously-variables shape parameters; 3) Introducing grain shape in numerical simulations with discrete element methods gives rise to various technical difficulties both geometrical and computational as for example contact detection and force calculation between particles of arbitrary shape [5].

This work is dedicated more precisely to the effect of one of these parameters - angularity - on the mechanical behavior of sheared granular packings. We first introduce our numerical approach in section 2, then, in Sect. 3, the shear strength behavior is presented for different values of angularity. The microstructure is analyzed in termes of network connectivity and force transmission in sect. 4 and 5 respectively

2 NUMERICAL PROCEDURES

The simulations were carried out by means of the contact dynamics method [1], which assumes perfectly rigid particles interacting through mutual exclusion and Coulomb friction. This numerical strategy, able to cope with stiff frictional contact laws, seems particularly relevant to address study of dense granular samples (even of large size) because it is not introducing numerical artifact due to contact stiffness. For this reason, the simulations can be performed with large time steps compared to molecular dynamics simulations. We used LMGC90 which is a multipurpose software developed in our laboratory, capable of modeling a collection of deformable or undeformable particles of various shapes by different algorithms.

Particles are constructed following a strict procedure in order to isolate and control precisely the shape. Firstly, a set of n_v vertex is randomly generated on the unit sphere. The convex hull of these points is created by associating three vertex for each faces. This condition imply that the number of face n_f is simply given by $n_f = 2n_v - 4$. Secondly, to be sure to avoid particle eccentricity, the degree η of distortion from a perfectly spherical shape, define as the ratio of the difference of the radius of subscribed and inscribed sphere over the radius of the subscribed sphere [9, 10] is computed. This parameter is similar to the *Sphericity* parameter used in soils mechanics. For nearly spherical particle we have $\eta < 0.1$. In other words, the first step is repeated until this condition was satisfied. We define thus the *angularity* α of a particle as the mean angle between touching faces of the polyhedra. In this simple way, for a given aspect ratio, we can control the angularity of the particles with a single continuously-variable shape parameters depending only to the number of faces n_f.

We prepare 6 different packings, named $S2$ to $S7$, each of them comprising 40,000 irregular polyhedra with the same number of faces n_f with $n_f \in [176, 96, 46, 30, 20, 8]$. The *packing angularity* $\langle\alpha\rangle$ is given by the mean angularity of the particles in the packing. In addition, we prepare a last packing $S1$, composed of spheres. In order to avoid long-range ordering, we introduce also a small size polydispercity by varying the diameter of the sphere circumscribing the particles. Figure 1 displays snapshots of the packings for

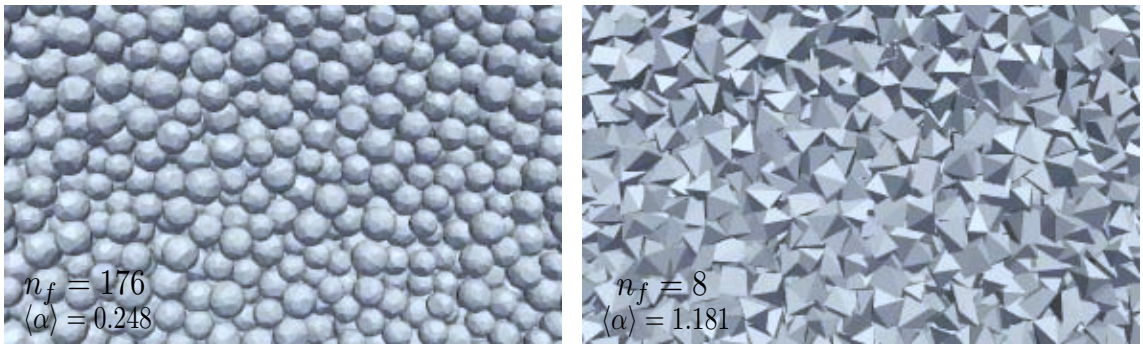

Figure 1: Examples of portion of the generated packings at the initial state.

two values of $\langle\alpha\rangle$ at the end of isotropic compaction presented below.

All samples were compacted by isotropic compression inside a box of dimensions $L_0 \times l_0 \times H_0$ in which the left, bottom and background walls are fixed and the top, the right and the front walls are subjected to the same compressive stress σ_0. The gravity was set to zero in order to avoid force gradients in the samples. The coefficient of friction was set to 0 between grains and walls during the isotropic compression. Thus, at equilibrium, all samples were in isotropic stress state. The isotropic samples are then subjected to vertical compression by downward displacement of the top wall at a constant velocity v_y for a constant confining stress σ_0 acting on the lateral walls. The friction coefficient μ between particles is set to 0.5 and to zero with the walls.

3 MACROSCOPIC SHEAR STRENGTH

The stress tensor $\boldsymbol{\sigma}$ can be evaluated from the simulation data as an average over all the contact of the dyadic product of contact force $\boldsymbol{f}^c$ and branch vector $\boldsymbol{\ell}^c$: $\sigma_{\alpha\beta} = n_c \langle f^c_\alpha \ell^c_\beta \rangle_c$ [1], where n_c is the number density of contacts c. Under triaxial conditions with vertical compression, we have $\sigma_1 \geq \sigma_2 = \sigma_3$, where the σ_α are the stress principal values. We extract the mean stress $p = (\sigma_1 + \sigma_2 + \sigma_3)/3$ and the stress deviator $q = (\sigma_1 - \sigma_3)/3$. The principal strain values are $\varepsilon_1 = \int_{h_0}^{h} dh'/h'$, $\varepsilon_2 = \int_{L_0}^{L} dL'/L'$ and $\varepsilon_3 = \int_{l_0}^{l} dl'/l'$. The cumulative shear strain is defined by $\varepsilon_q \equiv \varepsilon_1 - \varepsilon_3$

Figure 2(a) shows the normalized shear stress q/p as a function of shear strain ε_q for all values of $\langle\alpha\rangle$. The shear stress jumps initially to a high value before decreasing to a nearly constant value in the steady state. The steady-state shear stress $(q/p)^*$ characterizes the shear strength of the material. According to the Mohr-Coulomb model, in tri-axial geometry, the internal angle of friction, representing the shear strength of the material, is defined by $\sin\varphi^* = 3q/(2p+q)$ [6]. Interestingly, as shown by Fig. 2(b), the shear strength first increase with $\langle\alpha\rangle$ from 0.2 (spheres) and then saturate to $\simeq 0.4$ for the most angular shape. The saturation of φ^* suggests that, as $\langle\alpha\rangle$ increases, important changes occur in the grain-scale phenomena underlying macroscopic friction.

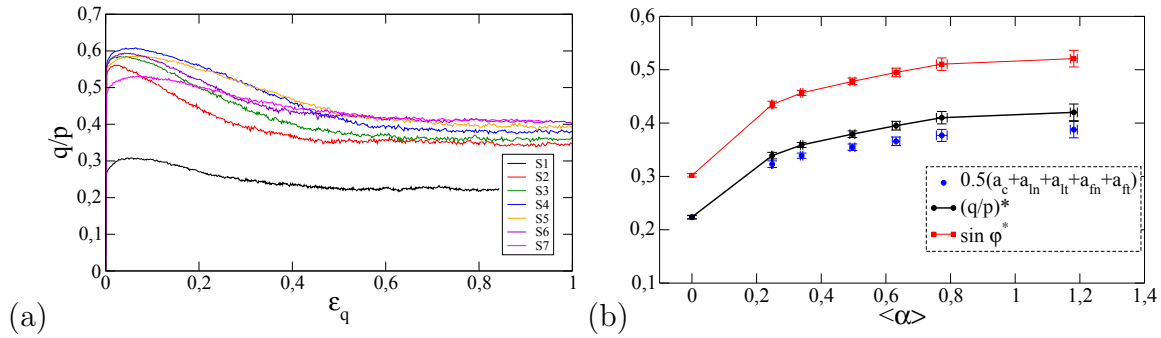

Figure 2: Normalized shear stress q/p (a) as a function of cumulative shear strain ε_q (b) averaged in the residual state together with the harmonic approximation and the friction angle $\sin\varphi$.

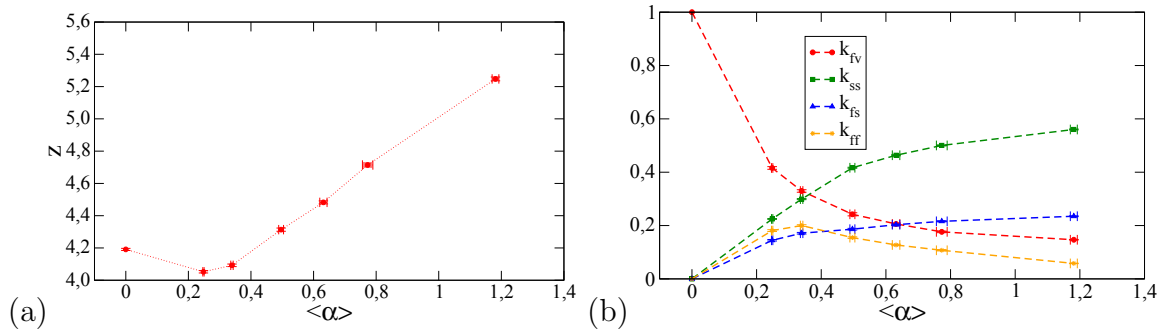

Figure 3: (a) Coordination number and (b) proportion of fv, ss, fs and ff-contacts, as a function of $\langle\alpha\rangle$ in the residual state.

4 CONTACT NETWORK CONNECTIVITY

The contact network can be characterized by the the coordination number z (average number of contacts per particle), which describe at the first order the connectivity of the packing. Figure Fig.3(a) shows z as functions of $\langle\alpha\rangle$ averaged in the residual state. We see that z increase from 4 to 5 with α showing that for large angularities, the packings are better connected. This can be attributed to the fact that sharp corners and sides, for most angular particles facilitate contacts with close neighbors that would be unreachable for rounder particles. This can be evidenced plotting the proportion of face-face (k_{ff}), face-side (k_{fs}), side-side (k_{ss}) and face-vertex (k_{fv}) as a function of $\langle\alpha\rangle$; Fig.3(b).

We see that k_{fv} decrease quickly from 1 (for spheres) to 0.15 with $\langle\alpha\rangle$. At same time, k_{ss} increase nearly symmetrically from 0 to 0.6. The proportion of fs contacts increases slightly to 0.2 whereas k_{ff} pass by a pic equal to 0.2 before declines to nearly 0.05. In this way, as the particle angularity increases, the packing passes from a contact network dominated by fv contacts to a contact network dominated by ss and fs contacts. The increasing connectivity of the particles is obviously correlated with the increase of shear strength due to the fact that face-side and side-side contacts are able to accommodate stronger forces chains than face-vertex contacts [7, 8].

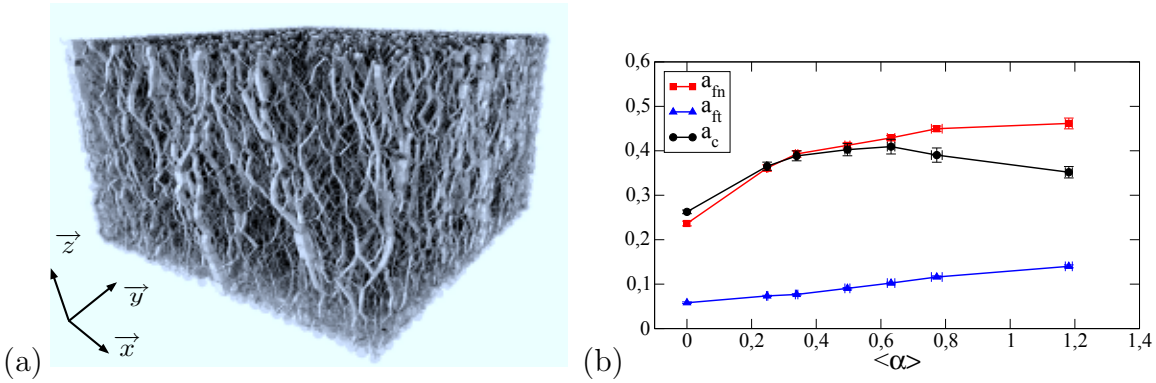

Figure 4: (a) Snapshot of radial forces in packing for S4 in the steady state. Line thickness is proportional to the radial force (b) contact and forces anisotropies, as a function of $\langle\alpha\rangle$ in the residual state.

5 TEXTURE AND FORCE TRANSMISSION

Figure 4(a) shows a typical map of radials forces in granular media (here for S4) highlighting the peculiar organization of forces. The force chains are clearly inhomogeneous forming anisotropic structures generally at the origins of shear strength. To analyze this anisotropic structures, a common approach used by various authors is to consider the angular distribution of contacts orientations $\boldsymbol{n}$, as well as the angular average of normal and tangential forces along the direction $\boldsymbol{n}$. In 3D, let $\Omega = (\theta, \phi)$ the azimutal and radial angles that define the orientations of $\boldsymbol{n}$. Under the axisymmetric conditions of our simulations, it is easy to see that each of this probability density functions are independent of the azimuthal angle ϕ. Moreover, under shearing, the packing self-organizes into a state where a simple approximations based on spherical harmonics at leading terms captures their anisotropies [2, 8]:

$$\left\{\begin{array}{lcl} P_\theta(\theta) & = & \frac{1}{4\pi}\{1 + a_c[3\cos^2(\theta-\theta_c) - 1]\}, \\ \langle f_n\rangle(\theta) & = & \langle f_n\rangle\{1 + a_{fn}[3\cos^2(\theta-\theta_{fn}) - 1]\} \\ \langle f_t\rangle(\theta) & = & \langle f_n\rangle a_{ft}\sin 2(\theta-\theta_{ft}), \end{array}\right. \tag{1}$$

where $\langle f_n\rangle$ is the mean normal force, a_c, a_{fn} and a_{ft} are the contact, normal force and tangential anisotropic parameters, and $\theta_c = \theta_{fn} = \theta_{ft} = \theta_\sigma$ the privileged directions of the corresponding angular direction coinciding with the principal direction of the shear stress. The anisotropies a_c, a_{fn} and a_{ft} are interesting descriptors of granular microstructure and force transmission properties, because they underlie the different microscopic origins of shear strength. Indeed, it can be shown that the general expression of the stress tensor leads to the following simple relation [2, 8]:

$$\frac{q}{p} \simeq \frac{5}{2}(a_c + a_{ln} + a_{lt} + a_{fn} + a_{ft}), \tag{2}$$

where a_{ln} and a_{lt} are the anisotropy of the mean orientation of the branch length projected along the normal and tangential direction, and where the cross products between the

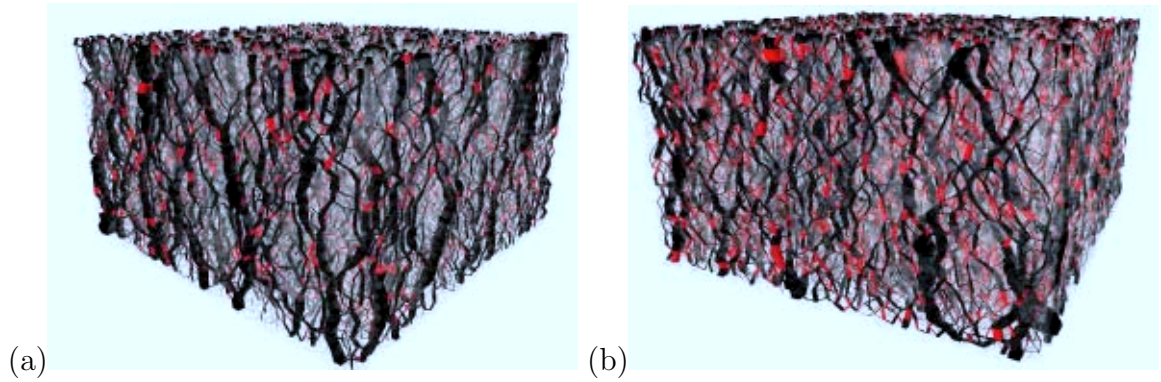

Figure 5: Snapshot of radial forces in packing for S3 (a) and S7 (b) in the steady state. Line thickness is proportional to the radial force. In red the force where $f_t = \mu f_n$.

anisotropy parameters have been neglected. In our simulation, due to the absence of shape eccentricity of the particles, we have $a_{ln} \sim a_{lt} \sim 0$. Figure 2(b) shows that Eq. 2 holds well for all values of $\langle\alpha\rangle$.

Figure 4(b) shows the variation of this three anisotropies as a function $\langle\alpha\rangle$. We see that a_c, a_{fn}, and a_{ft}, first increase with $\langle\alpha\rangle$, underlying the increase of the shear strength. This is a consequence of the increasing number of face-face, side-side and face-side contacts, which allow the force chains to be much more stable. Then, for $\alpha \gtrsim 0.5$ there is a decrease of a_c compensated by a increase of a_{ft} whereas a_{fn} remains constant, which explains the strength plateau shown in Fig. 2. This happens because very angular particles also have very few faces, so that it becomes difficult to orient these faces perpendicularly to the direction in which the forces are being transmitted. This causes the anisotropies a_c to decrease. In addition, a_{ft} increases, since the stability of such contacts relies on a strong activation of friction forces [8, 9, 10]. This is well illustrated inFig. 5 where a map of mobilized forces (ie $f_t = \mu f_n$) are shown in red for S3 (a) and for S7) (b).

6 DISCUSSIONS AND CONCLUSIONS

In this paper, we applied the contact dynamics method to simulate large samples of polyhedral particles. The angularity of the particles is controlled by varying the number of the face of the polyhedra. It was shown that the shear strength first increases with the angularity and then remains nearly constant at larger angularity. For high angularities, the plateau of shear strength results from a decrease of the contact anisotropies compensated by an increase of the tangential force anisotropy. This transition results from a geometric effect that becomes dominant for very angular particles (a few number of faces along the stress direction) and that implies that the stability of the packing relies strongly on friction forces (particles are better surrounded).

Nevertheless, much more work is needed in order to understand the mechanical role of each contact type on the stress transmission. An idea is to isolate the contribution of each contact on the texture and forces anisotropies. On other way, a well known result

of idealized granular media is that the contacts can be classified into strong and weak networks with distinct mechanicals role. It will be interesting to revisit this concept for our angular particles. This investigation are underway and they will be presented in forthcoming publication.

REFERENCES

[1] Moreau, J.-J,. Some numerical methods in multibody dynamics: application to granular materials. *Eur. J. Mech. A/Solids.* (1994) **13**:93-114.

[2] Ouadfel, H., Rothenburg, L. 'Stress-force-fabric' relationship for assemblies of ellipsoids. *Mechanics of Materials.* (2001) **33**:201-221.

[3] Mirghasemi, A., Rothenburg, L., and Maryas, E. Influence of particle shape on engineering properties of assemblies of two-dimensional polygon-shaped particles. *Geotechnique.* (2002) **3**:209.

[4] Donev, A., Stillinger, F., Chaikin, P. and Torquato, S. Unusually Dense Crystal Packings of Ellipsoids. *Phys. Rev. Lett.* (2004) **92**: 255506.

[5] Nezami, E.G., Hashash, Y.M.A., Zhao, D. and Ghaboussi, J. A fast contact detection algorithm for 3-D discrete element method. *Computers and Geotechnics* (2004) **31**: 575-587.

[6] Mitchell, J.K., Soga, K. *Fundamentals of Soil Behavior*. Wiley, New York (2005).

[7] Azéma, E., Radjai, F., Peyroux, R. and Saussine, G. Force transmission in packing of pentagonal particles. *Phys. Rev. E.* (2007) **76**:011301.

[8] Azéma, E., Radjai, and Saussine, G. Quasistatic rheology, force transmission and fabric properties of a packing of irregular polyhedral particles. *Mechanics of Materials* (2009) **41**:729-741.

[9] Azéma, E. and Radjai, F., Stress-strain behavior and geometrical properties of packings of elongated particles. *Phys. Rev. E.* (2010) **81**: 051304.

[10] Saint-Cyr, B., Delenne, J.-Y., Voivret C., Radjai, F. and Sornay, P. Rheology of granular materials composed of nonconvex particles. *Phys. Rev. E.* (2010) Submited.